ELSEVIER

Journal of Photochemistry and Photobiology A: Chemistry 143 (2001) 229–240

Journal of Photochemistry and Photobiology A:Chemistry

www.elsevier.com/locate/jphotochem

An active, robust and transparent nanocrystalline anatase TiO_2 thin film — preparation, characterisation and the kinetics of photodegradation of model pollutants

R. Fretwell*, P. Douglas

Chemistry Department, University of Wales Swansea, Singleton Park, Swansea SA2 8PP, UK

Received 11 July 2001; accepted 17 July 2001

Abstract

The preparation, characterisation, and photocatalytic activity of robust and transparent nanocrystalline thin films of anatase TiO_2 are described. The films, which are prepared from a sol–gel can be either dip-coated or spin-coated, however, the latter have better optical and mechanical properties, since dip coating results in the retention of a significant amount of the organic stabilisers used in the sol–gel preparation.

Quantum yields for the photooxidation of 4-chlorophenol (Φ_{4CP}) on these spin-coated films are similar to those reported previously for TiO_2 films and dispersions, with $\Phi_{4CP} = 0.5$–1%. For films of different thicknesses, and therefore different absorption efficiencies, Φ_{4CP} depends only upon the total number of photons absorbed, i.e. Φ is independent of both the absorbed photon flux and the distribution of charge carriers in the film. By way of contrast, the rate of photoreduction of methylene blue is independent of film thickness and appears to be limited by the surface area of the film. Hence, quantum yields for methylene blue reduction (Φ_{MBR}) fall significantly from 1.7 to 0.5% as film thickness, and hence photoabsorption efficiency, is increased. These pure anatase films do not show any deleterious sodium ion effect for either 4-chlorophenol oxidation or methylene blue reduction. Quantum yields for photooxidation of stearic acid (Φ_{SA}) deposited directly onto the films are relatively high with $\Phi_{SA} = 1$–4%. This, combined with the excellent optical and mechanical properties of these films, suggests that they may be of particular interest for the development of 'self-cleaning windows'.

Keywords: TiO_2; Nanocrystalline; Photodegradation; 4-Chlorophenol; Methylene blue; Stearic acid

1. Introduction

The photocatalytic behaviour of TiO_2 has been, and continues to be, the subject of much research. A great deal of this has been directed at its use in applications involving the photoreactions of organic materials, in particular the photodestruction of organic pollutants [1], 'self-cleaning windows' [2–4], and photocatalysis of organic compounds in the solid [3,5–8], liquid [9–19], and gas [10,20–25] phases.

In the field of pollutant removal much work has been done with phenol, chlorophenols and related compounds [13–19] with 4-chlorophenol receiving attention as a standard compound for studies with TiO_2 dispersed as a slurry [26–34] or deposited on glass as a thin film [13–18]. Methylene blue (MB), which can be both photooxidised and photoreduced on TiO_2 if irradiations are carried out under the appropriate conditions, has also been the subject of much work [35–38]. Methylene blue has two desirable features for these studies, i.e. a high visible wavelength extinction coefficient, which allows the use of low concentrations and easy monitoring of photoreactions, and reasonable transparency to the band of UV light most often used for irradiation of TiO_2. Studies with TiO_2-coated 'self-cleaning windows' have used stearic acid [3,5–7] and palmitic acid [8], which are found in natural greases, as convenient test materials. It should be noted, however, that extrapolation of photodegradation behaviour from one compound, and/or degradation route, to another must be made with caution [1].

In recent years research into semiconductor photocatalysis has been largely dominated by the development of "nanocrystalline" TiO_2 thin films [1,39] which are transparent and scatter less light than the Degussa P25 TiO_2 used previously. These nanocrystalline films have been shown to be as photochemically active as, and more physically and chemically robust than, the 'standard' Degussa P25 films [24].

* Corresponding author. Tel.: +44-1792-205678/ext. 4205; fax: +44-1792-295747.
E-mail address: cmsolar@swansea.ac.uk (R. Fretwell).

1010-6030/01/$ – see front matter
PII: S1010-6030(01)00526-3

In this work we wish to report the preparation and physical characterisation of a particularly robust and transparent nanocrystalline TiO_2 film, together with results from kinetic studies of the photodegradation of 4-chlorophenol, methylene blue, and stearic acid using this material.

2. Experimental

2.1. Materials

Chemicals were obtained as follows. Ethanol (synthetic grade), methanol (analytical reagent grade), nitric acid, and sulphuric acid, from Fisher Chemicals; polyethylene glycol 600, titanium isopropoxide ($Ti(OCH(CH_3)_2)_4$), and stearic acid from Aldrich; diethylene glycol (>98%) from Fluka; P25 TiO_2 from Degussa; nitrogen (oxygen-free), argon and oxygen, from BOC gases.

2.2. Film preparation

The substrates used as film supports were either standard sodaglass microscope slides ~1 mm thick (BDH), Pilkington conducting 'K' glass which is 4 mm thick and coated with fluorine doped SnO_2 on one side, or quartz. All were rinsed in nitric acid prior to use.

2.3. Preparation of sol

Sols were prepared, using a previously published method, by the hydrolysis of titanium isopropoxide in the presence of polyethylene glycol (PEG) and diethylene glycol (DEG) to prevent the aggregation of the titania particles produced [23]. An amount of 2.5 g of PEG and 2.5 g of DEG, were dissolved in 40 ml of ethanol and 5 g of $Ti(OCH(CH_3)_2)_4$ was added quickly and with stirring to give a transparent, colourless, liquid which is stable for several months if stored under nitrogen.

2.4. Dip coating

The glass supports were dipped in the solution by hand in a glove bag filled with nitrogen in an atmosphere of less than 5% humidity. After each coat the film was allowed to dry at room temperature and then calcined at 450°C in a furnace for 30 min.

2.5. Spin coating

The spin coater used was a Model 4000 from Electronic MicroSystems Ltd. An amount of 100 μl of solution was spun on a piece of 2.5 cm × 0.9 cm glass at a speed of 1250 rpm for 20 s under a stream of nitrogen and allowed to dry at room temperature. (An examination of the effect of varying spin coating speed from 1000 to 7500 rpm showed no dependence of film characteristics upon spin coating speed.) When dry the film can be left in air and will remain transparent. However, it can be easily removed from the glass substrate by wiping with a little ethanol, and therefore even after casting, the geometry and size of the film can be altered. Films were then calcined at 450°C for 30 min in a furnace, after which the films were resistant to abrasion.

2.6. Effect of calcining temperature

Calcining the film results in much improved mechanical properties. Films calcined at temperatures below 100°C are not robust, do not adhere well to the glass substrate, and flake off from the glass substrate into the solution. Calcining at 200°C gives a film that can be removed from the glass substrate by scratching with a thumbnail. Films calcined at 450°C are robust while calcining at temperatures above 450°C is not practical since at these temperatures the glass substrate begins to soften.

2.7. P25 films

These were prepared using a wash coat method with a 5% slurry in water, and dried at 100°C for 1 h after each coat [14].

2.8. Other films

The film prepared following the method of Grätzel [40] was supplied by Johnson Matthey Technology Centre, Reading, UK.

2.9. Irradiations

Irradiations were carried out using a cylindrically reflective irradiation chamber lined with 12, 8 W UVA (320–390 nm, λ_{max} at 355 nm) black light tubes supplied by Coast Air. The sample was placed in a thermostated cell (30°C) at the centre of the irradiation chamber. Absolute quantum yields were obtained using ferrioxalate actinometry [41]. The incident photon flux from one direction on an area of 2.5 cm × 0.9 cm (the size of the TiO_2 slides used) was 3.5×10^{15} photons s^{-1}. The photon flux transmitted through one direction by a 2.5 cm × 0.9 cm seven-coat spin-coated film was 1.85×10^{15} photons s^{-1}; i.e. an absorbed photon flux of 1.65×10^{15} per slide (0.73×10^{15} photons cm^{-1} s^{-1}) when irradiated from one direction. During photodegradation experiments the cell was irradiated from both sides to give an absorbed photon flux for a seven-coat spin-coated film of 3.3×10^{15} photons s^{-1}. Absorbed photon fluxes for other slides were calculated from this data together with the emission spectrum of the lamp and the absorption and light scattering characteristics of the films.

2.9.1. 4-Chlorophenol

One TiO_2 slide was placed in a microfluorescence cell (internal dimensions 4 mm × 10 mm × 40 mm) with 1 cm^3

of a solution of 10^{-3} M 4-chlorophenol in water acidified to pH 2 with $HClO_4$. Oxygen was bubbled gently through the cell both before (15 min) and during irradiation. Absorbance readings were recorded at λ_{max} of 4-chlorophenol which is 280 nm ($\varepsilon = 1500\,mol^{-1}\,dm^3\,cm^{-1}$). In studies with films prepared on the 4 mm Pilkington K glass a 1 cm path length (10 mm × 10 mm × 40 mm) fluorescence cell was used together with a glass block inserted to make the internal dimensions the same as those of the microcell.

2.9.2. Methylene blue

For reduction, one TiO_2 slide was placed in a 1 cm path length fluorescence cell with 2.5 cm^3 of a solution of 10^{-5} M methylene blue in 20:80 v/v methanol/water, acidified to pH 2 with $HClO_4$ (the methanol acts as a sacrificial electron donor) [35]. The cell was purged with argon in darkness for 15 min prior to illumination and then throughout the irradiation. For oxidation, a 10^{-5} M solution of MB in distilled water was used and the sample was purged with oxygen, before and during irradiation. Absorbance readings were recorded at 665 nm which is λ_{max} for MB, with $\varepsilon = 1 \times 10^5\,mol^{-1}\,dm^3\,cm^{-1}$ [35].

2.9.3. Treatment of glass to investigate sodium ion effects

The acid treatment of the glass consisted of rinsing in 2-propanol, boiling for 30 min in 70% H_2SO_4, and finally rinsing thoroughly in double distilled water [3]. Following spin coating the slides were calcined at 450°C for 30 min.

2.9.4. Photodegradation of stearic acid

Experiments on the photodegradation of stearic acid were carried out using 2.5 cm × 2.5 cm spin-coated TiO_2 slides carrying either one or seven coats of TiO_2. These were then coated with pure stearic acid by spin coating a film of stearic acid from a methanolic (8.8×10^{-3} M stearic acid) solution followed by drying under a stream of nitrogen. Photodegradation was followed by FT-IR in the 2700–3000 cm^{-1} spectral region [3,5] using a Mattson Instruments Satellite FT-IR. Quantification of the IR absorbance data was obtained by reference to published data obtained with stearic acid films of known thicknesses [5] which gave an absorbance of 0.010 at 2915 cm^{-1} for five monolayers of stearic acid at a thickness of 12.5 nm.

2.9.5. XRD, SEM and TEM data

X-ray diffraction (XRD), scanning electron microscopy (SEM), and transmission electron microscopy (TEM) were all carried out at Johnson Matthey Technology Centre, Reading, UK. The instruments used were as follows. XRD: Siemens D500 $\theta/2\theta$-coupled, fitted with a single sample holder (samples were analysed whilst attached to the glass substrate). SEM: Leica S440i (samples sputtered with carbon prior to analysis, films analysed on the glass substrate). TEM: Philips EM400T (samples of TiO_2 films scraped off the glass support with a scalpel and dispersed in isopropanol in a sonic bath prior to mounting and analysis).

3. Results and discussion

3.1. Film characterisation

3.1.1. Robustness

Both dip-coated and spin-coated films were resistant to peeling with adhesive Scotch Tape™ and scratching with pencil points of 2H hardness [3], and were not removed from the glass substrate even with 1 M NaOH. In comparison, P25 films can be removed by wiping with a damp cloth, and a film supplied by Johnson Matthey Technology Centre, Reading, UK, prepared using the method of Grätzel [40] could be destroyed by scratching with pencil points. Dip coating gave inferior films to spin coating. When prepared by dip coating, cracking occurred both on the film surface and at the edges of the film where the solution had drained (Fig. 1). This was particularly noticeable with multi-coated films where it gives rise to films which show significantly higher light scattering than the spin-coated analogues (Fig. 2).

3.1.2. UV–VIS spectroscopy

Fig. 2 shows absorption spectra for dip-coated and spin-coated films at various thicknesses. Both films show much lower scattering than films made using P25 TiO_2, and the spin-coated films show a sharper absorption band edge, and lower visible absorption/scattering, than their dip-coated analogues. For optical applications the excellent transparency of these spin-coated films is a very desirable feature.

3.1.3. XRD, TEM and SEM data

3.1.3.1. Spin-coated nanocrystalline films. XRD data for a seven-coat nanocrystalline film showed it to be pure anatase with a fundamental crystallite size of 12–30 nm. TEM showed angular crystallites 8–30 nm across held in dense clusters with no evidence of residual organic material (Fig. 3).

3.1.3.2. Dip-coated nanocrystalline films. The film thickness of a seven-coat film was found to be 190 ± 20 nm from SEM. XRD revealed the crystal phase as anatase, with a fundamental crystallite size of 12–30 nm. TEM data confirmed this crystallite size, and revealed, in addition, a high content of organic stabiliser (PEG and DEG) still present. The organic content was found to be highest at the edge of the films where the sol had drained during drying.

3.1.3.3. P25 film. The film thickness of the three-coat P25 film was found to be 2.3 ± 0.2 mm, almost 10 times thicker than the nanocrystalline film. XRD showed a phase distribution of 70:30 anatase:rutile, with crystallites 25 nm (anatase) and 36 nm (rutile) across.

The surface of the spin-coated nanocrystalline films is very smooth, with no structure apparent even at 20,000×

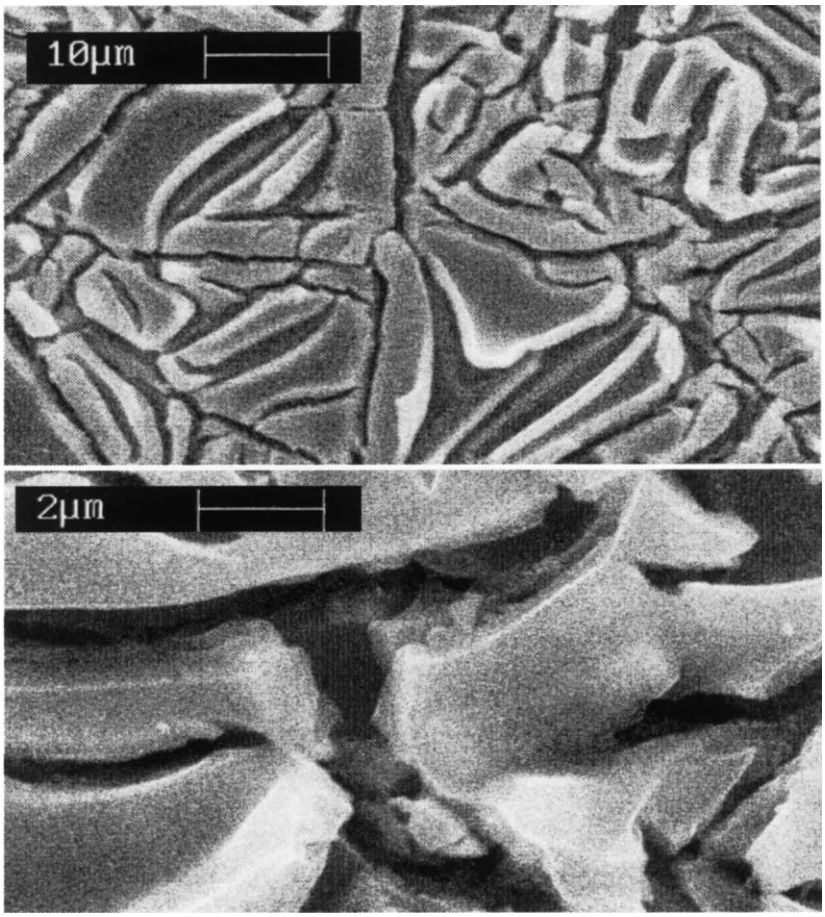

Fig. 1. Scanning electron micrograph of a 10-coat dip-coated film at 1000× (top) and 5000× (bottom) magnification. Substantial cracking is seen upon the film surface.

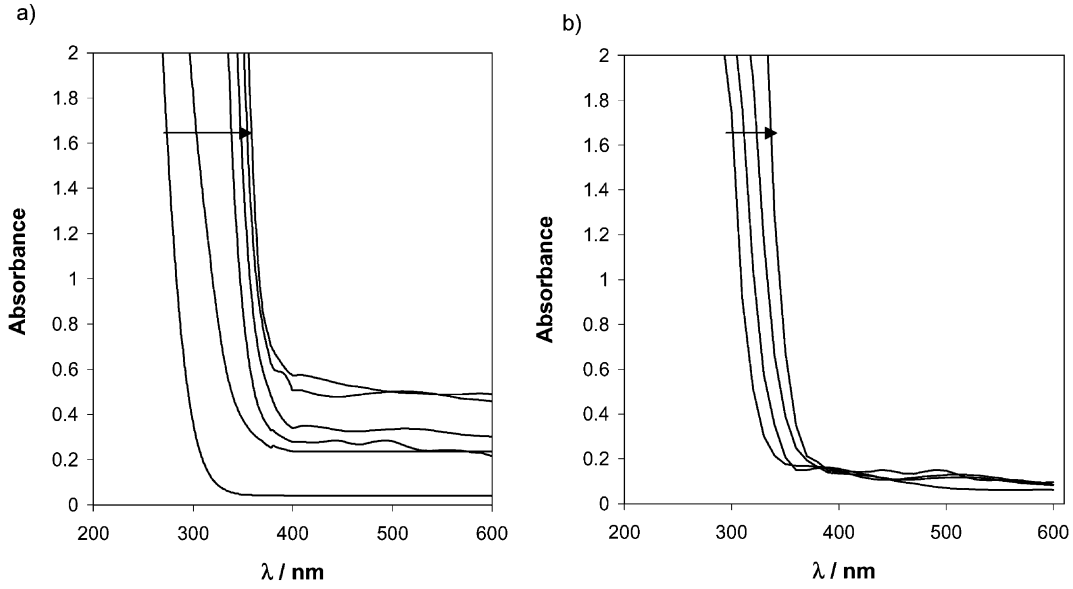

Fig. 2. Absorption spectra of a series of nanocrystalline TiO_2 films prepared using (a) dip coating (number of coats from 0, 1, 3, 5, 7 and 10 in direction of arrow), and (b) spin coating (number of coats from 1, 3, 5 and 7 in direction of arrow). The apparent absorption of dip-coated films above ca. 400 nm is due to light scattering.

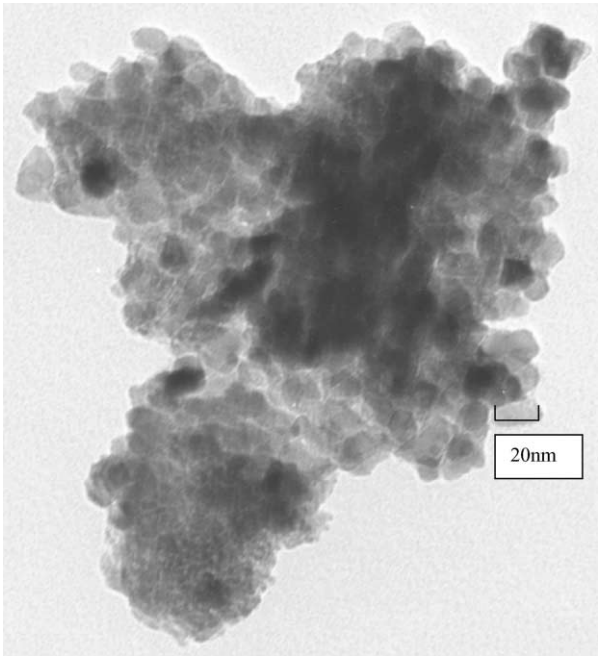

Fig. 3. A TEM micrograph showing the crystallites of TiO_2 found in the seven-coat spin-coated film to be within the range 8–30 nm. No residual organic stabiliser is present in this case.

magnification. In contrast, the surface of the P25 layer shows a rough structure even at 5000× magnification (Fig. 4).

3.2. Photodegradation studies

3.2.1. 4-Chlorophenol

The loss in absorbance at λ_{max} of 4-chlorophenol (280 nm) as a function of (a) irradiation time and (b) total absorbed photons for spin-coated films of different thicknesses, and hence different absorption efficiencies, is shown in Fig. 5a and b. The decay kinetics for *loss of absorbance* are complex and appear to include both an induction period and autocatalysis. This makes comparisons of quantum yields difficult because they vary with the extent of reaction, i.e. the total number of photons absorbed. However, as Fig. 5b shows the extent of reaction depends only upon the total number of photons absorbed and is independent of the rate of photon absorption by the film. Upon reaching seven coats an increase in the number of TiO_2 coats no longer resulted in an increase in photodegradation rate under our irradiation conditions. This is in agreement with the observed spectral properties which show that coating more than seven coats leads to no significant increase in

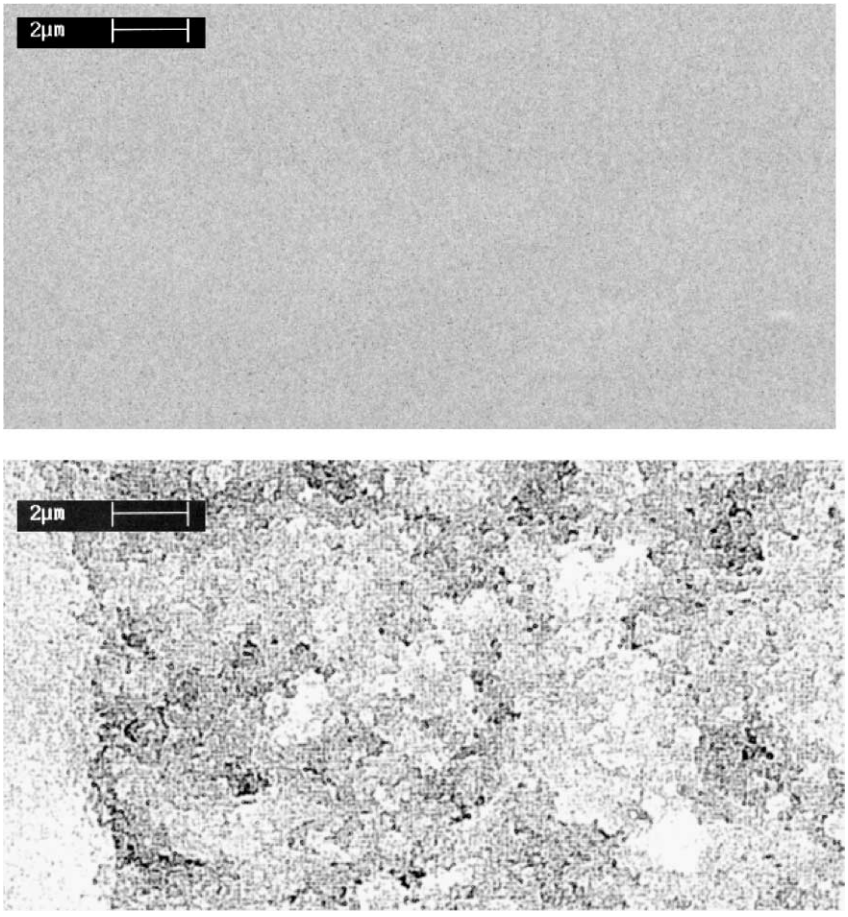

Fig. 4. SEM of a seven-coat spin-coated film (top), and a three-coat P25 film (bottom). The surface of the former is very smooth in comparison to the rough structured P25 film.

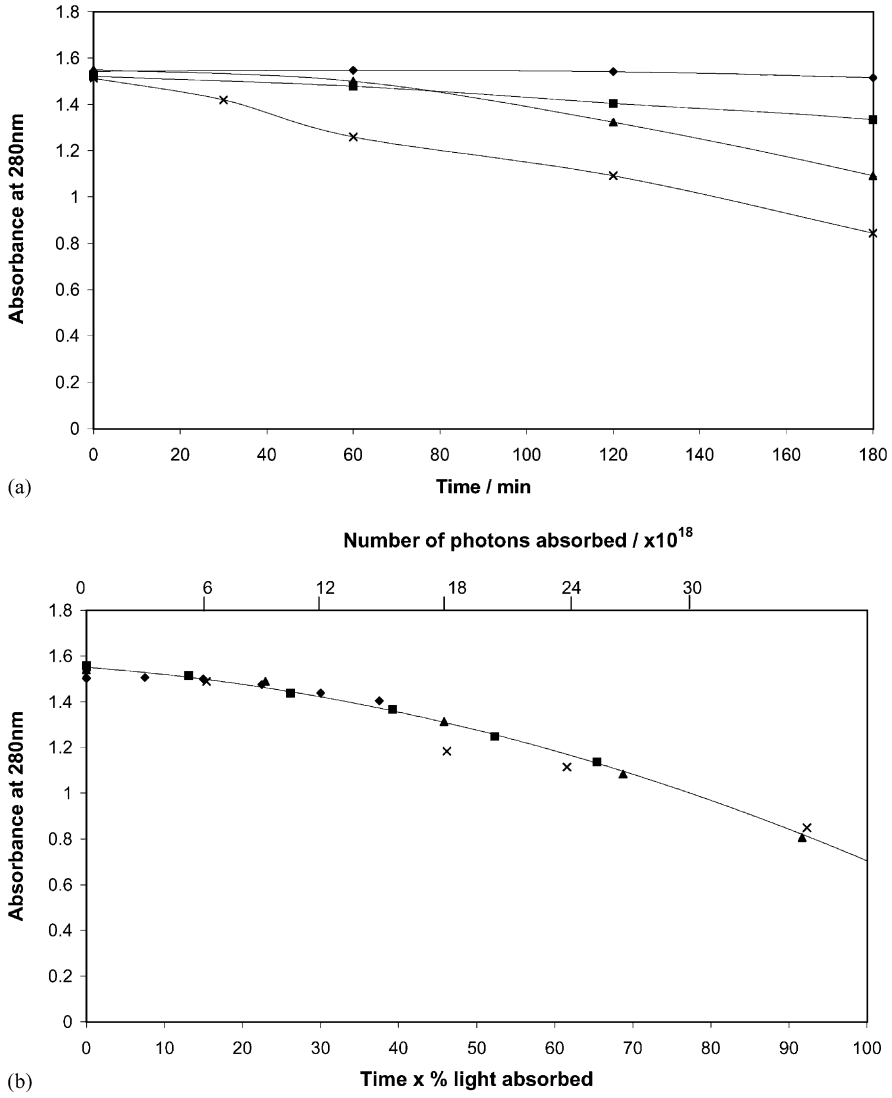

Fig. 5. (a) Loss in absorbance at 280 nm for the degradation of 4-chlorophenol using spin-coated slides with varying numbers of coats: 1 (◆, 13% light absorbed); 3 (■, 22%); 5 (▲, 38%); 7 (×, 51%). (b) Loss in absorbance at 280 nm as a function of total absorbed photons for the photodegradation of 4-chlorophenol using spin-coated films: 1 (◆); 3 (■); 5 (▲); 7 (×) coats.

absorption of light from the black light lamps. Parallel data for dip-coated slides are shown in Fig. 6a and b. Fig. 7 shows comparative data for spin-coated nanocrystalline (seven coats), dip-coated nanocrystalline (seven coats), Degussa P25, and the film prepared following the method of Grätzel [40].

Table 1 collects minimum quantum yields for different film preparations at three different values of total number of absorbed photons. These quantum yields are calculated on the basis that all absorption at 280 nm is due to 4-chlorophenol and are, therefore, minimum values since any absorption of light at 280 nm by intermediate products will cause an underestimation of the quantum yield.

Although there is no measurable difference in the photocatalytic activity of spin-coated and dip-coated nanocrystalline films, the spin-coated films have much better transparency, and lower absorption, in the visible region.

3.2.2. Methylene blue

3.2.2.1. Photoreduction and photooxidation. Studies of methylene blue photodegradation were restricted to spin-coated nanocrystalline TiO_2 and dip-coated P25 films. Degradation profiles under reducing conditions using spin-coated nanocrystalline TiO_2 films with different numbers of coats of TiO_2 are shown in Fig. 8. The initial rates are very similar for all coatings even though the absorbed photon flux is different in each case. Fig. 9 shows the variation in initial photoreduction rate as a function of the number of coats of TiO_2 used in preparing the

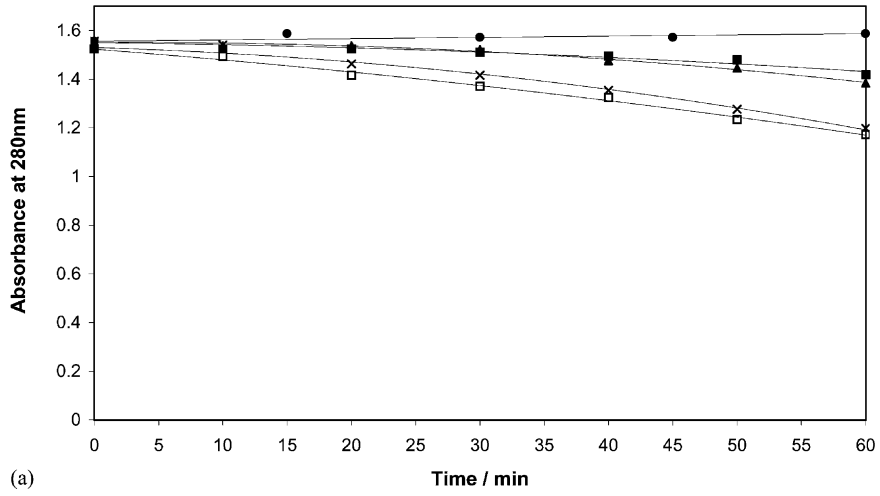

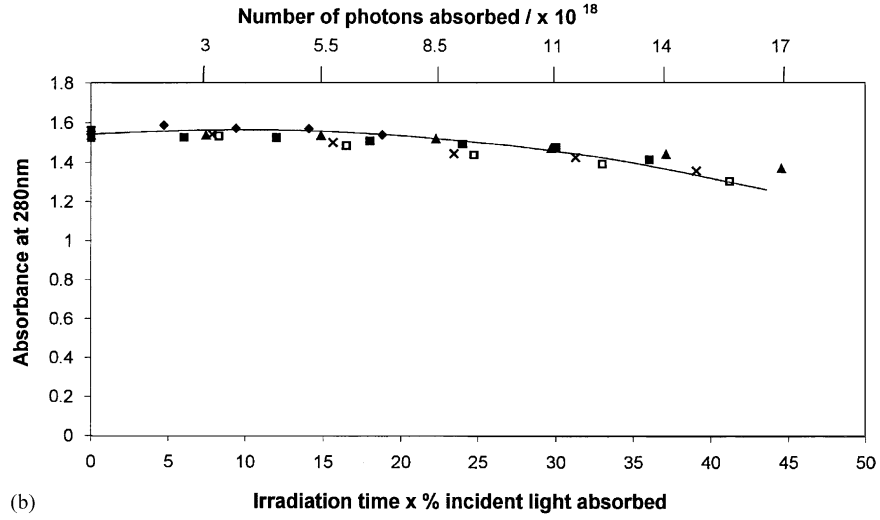

Fig. 6. (a) Loss in absorbance at 280 nm for the photodegradation of 4-chlorophenol using dip-coated slides with 0 (●), 3 (■, 60% light absorbed), 5 (▲, 74%), 7 (×, 78%), and 10 (□, 82%) coats of TiO_2. (b) Loss in absorbance of 4-chlorophenol at 280 nm as a function of total absorbed photons for dip-coated films: 1 (◆); 3 (■); 5 (▲); 7 (×) and 10 (□) coats.

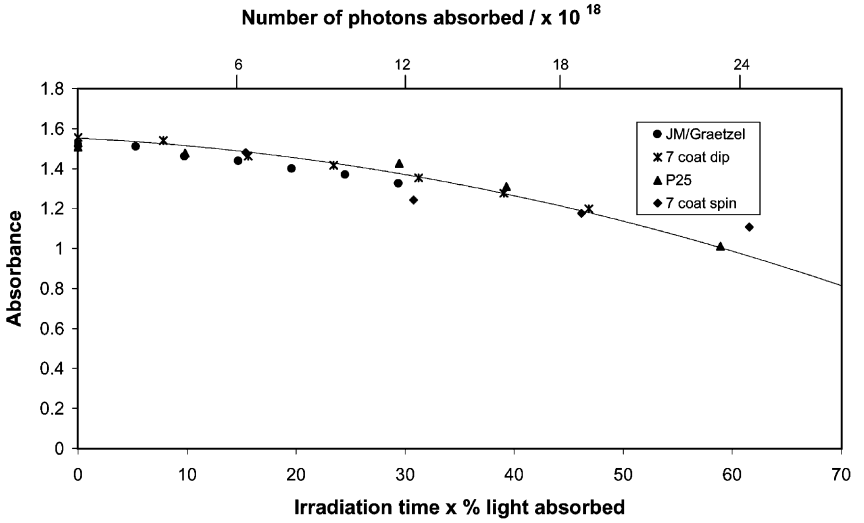

Fig. 7. Loss in absorbance at 280 nm using four different TiO_2 films as a function of total number of photons absorbed for the degradation of 4-chlorophenol.

Table 1
Quantum yields for varying film preparations at given photon absorptions

Type of film	Total number of photons absorbed					
		$\Phi \times 10^3$ (±1.0)		$\Phi \times 10^3$ (±1.0)		$\Phi \times 10^3$ (±1.0)
Spin	6×10^{18}	2.8	12×10^{18}	7.4	18×10^{18}	8.5
Dip	6×10^{18}	6.0	13×10^{18}	6.5	19×10^{18}	7.5
P25	4×10^{18}	2.6	16×10^{18}	4.9	23×10^{18}	9.0
JM	6×10^{18}	5.9	12×10^{18}	6.9	–	–

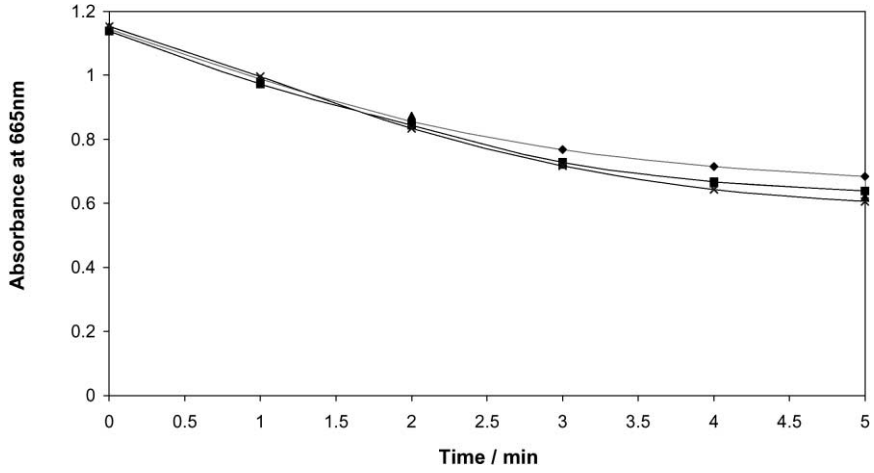

Fig. 8. Photoreduction of methylene blue using a series of spin-coated nanocrystalline TiO_2 films: 1 (◆, 12% light absorbed); 3 (■, 22%); 5 (▲, 38%); 7 (×, 51%) coats.

slides together with quantum yields as a function of the percentage of light absorbed. It is interesting to note that, in contrast to the results found for the photodegradation of 4-chlorophenol, the photoreaction efficiency is essentially independent of the number of coats used in preparing the film. The observations that the rate of photoreduction of methylene blue is independent of film thickness, and that quantum yields fall significantly as film thickness (and hence photoabsorption efficiency) is increased, suggest that the reaction is controlled by the irradiated area of TiO_2 available for adsorption by reactants. This suggestion is supported by the high quantum yield obtained when using a P25 film, which has a much rougher surface than those prepared using nanocrystalline titania (see Fig. 4).

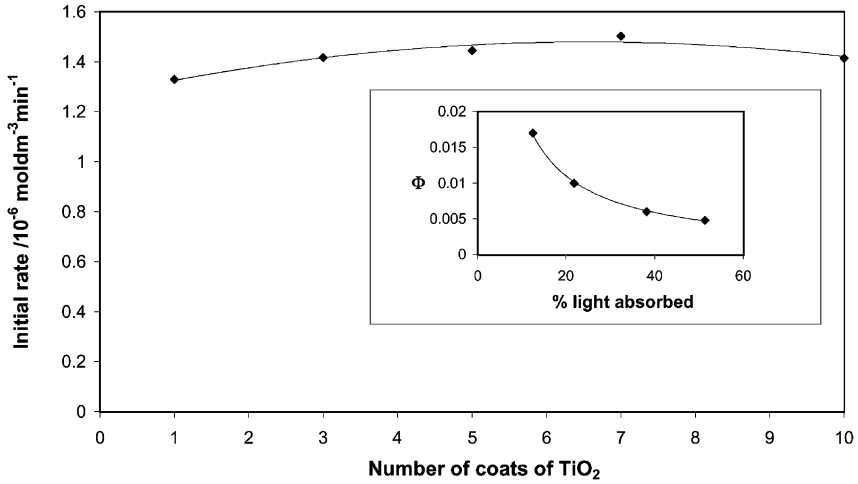

Fig. 9. The effect of number of coats of TiO_2 on the initial rate of photoreduction of methylene blue. Rate measured using the loss in absorbance at 665 nm of 10^{-5} M methylene blue at pH 2 with 20:80 v/v methanol/water over a 3 min irradiation period. Insert: quantum yield for the photoreduction of MB vs. the absorption efficiency.

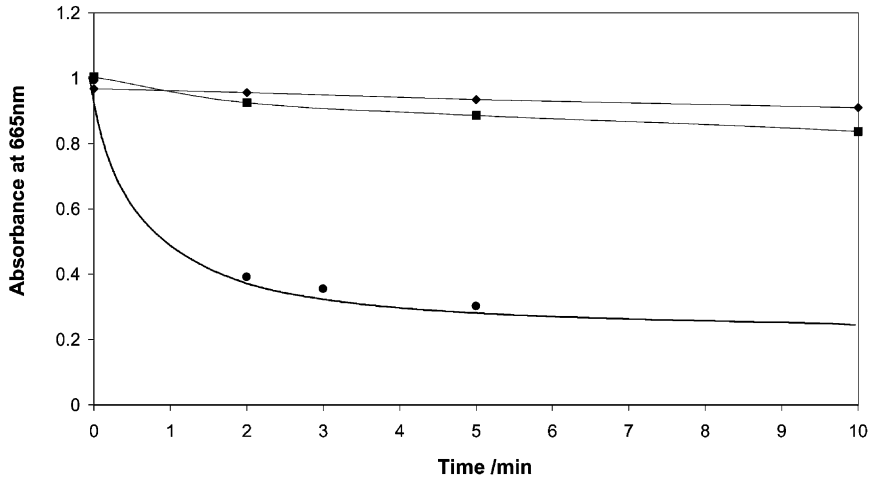

Fig. 10. Photooxidation profiles of methylene blue using three different films: one-coat spin-coated nanocrystalline film (◆); seven-coat spin-coated nanocrystalline film (■); three-coat P25 film (●).

Degradation profiles for photooxidation using one-coat and seven-coat spin coat are shown in Fig. 10 with data for a P25 film for comparison. Table 2 collects appropriate quantum yields.

Examination of the data in Tables 1 and 2 highlights the dangers of trying to generalise the photocatalytic activity of TiO_2 from one test reactant to another, or even from one reaction to another with the same compound. The photokinetic behaviour of the TiO_2/MB system under reducing conditions is completely different to either TiO_2/MB or TiO_2/4-chlorophenol under oxidising conditions. And for MB and 4-chlorophenol oxidation the relative rates with nanocrystalline and P25 TiO_2 vary considerably.

Table 2
Quantum yields for the photoreduction and photooxidation of methylene blue

Film type	Initial quantum yields	
	MB photoreduction	MB photooxidation
One-coat spin	0.017	0.0025
Three-coat spin	0.010	–
Five-coat spin	0.006	–
Seven-coat spin	0.005	0.0021
JM/Grätzel	0.006	–
P25	0.044	0.048[a]

[a] This is the integrated quantum yield over 2 min, the initial quantum yield may be as much as three times higher (see Fig. 10).

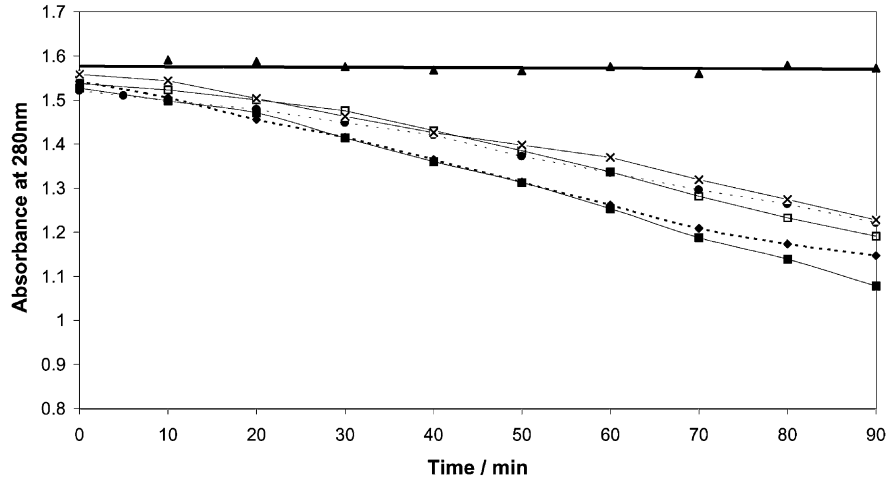

Fig. 11. Loss in absorbance at 280 nm for the photodegradation of 4-chlorophenol using seven-coat spin-coated films deposited on coated untreated (■), and coated treated (◆) microscope slides; 4 mm conduction glass treated (●), and untreated non-conducting side (□) and untreated conducting side (×). All seven-coat spin-coated films. Also shown are data for a treated blank slide (▲).

Table 3
Quantum yield data for studies of sodium ion effects using various substrates

	Φ
Quantum yields for 4-chlorophenol degradation calculated from a 60 min irradiation	
Microscope slide untreated	0.0100
Microscope slide treated	0.0093
Conducting glass (SnO_2-coated)	0.0072
Conducting glass reverse	0.0076
Conducting glass reverse treated	0.0066
Quantum yields for methylene blue reduction calculated from a 3 min irradiation	
Untreated one-coat microscope slide	0.014
Treated one-coat microscope slide	0.016
Quartz	0.014

3.2.3. Sodium ion effects

It has been suggested by Heller and co-workers [3,42] that migration of sodium oxide from a sodaglass substrate into TiO_2 films causes a reduction in photocatalytic activity. In his work he suggests that by treating the glass with acid to remove surface sodium the photoactivity of the film can be improved by factors of between 3 and 10 depending on the conditions. We have examined this phenomena using a variety of substrates, i.e. sodaglass, for which a sodium ion effect might be expected; Pilkington K glass, one side of which has a coating of fluorine doped SnO_2 on the surface which may be expected to act as a barrier to sodium migration; and quartz. Fig. 11 and Table 3 show the results from this study with respect to both 4-chlorophenol degradation and methylene blue photoreduction. As the results show there is no detectable 'sodium ion effect' with these films. This is not altogether surprising since XRD shows that the TiO_2 phase for all films reported here are exclusively anatase, and the sodium ion effect would appear to be a consequence of a change in phase from anatase to brookite (or an incompletely characterised phase) [3] associated with the migration of sodium ions into TiO_2 films.

3.2.4. Stearic acid

One application for which the good photocatalytic activity and excellent transparency of the spin-coated nanocrystalline TiO_2 films is particularly appropriate is the removal of organic residues on window glass. Fig. 12 shows IR absorption spectra in the C–H stretching region (2800–3000 cm^{-1}) for the photodegradation of an 88 nm thick film of stearic acid, which was overcoated onto a seven-coat TiO_2 film. Irradiation results in a drop in the intensity of the C–H absorption bands as the C–H bonds are lost during oxidation of stearic acid to H_2O and CO_2. Fig. 13 shows rate data for loss of the C–H adsorption for one-coat and seven-coat films under identical irradiation conditions.

The highly non-linear decay curve observed for stearic acid degradation with the seven-coat film results in time-dependent quantum yields. A comparison of initial quantum yields for stearic acid degradation (Φ_{SA}), gives $\Phi_{SA} = 0.0082$ for the one-coat film, and 0.033 for a seven-coat film, while the integrated quantum yield for a seven-coat film over 10 min irradiation is 0.01. These compare with values of 0.00026 for the 'formal quantum efficiency' at 365 nm, and 0.00165 absolute quantum efficiency at 254 nm measured by Paz et al. [3] for another nanocrystalline film. It takes 26 molecules of oxygen, and the transfer of 104 electrons, for the complete oxidation of one molecule of stearic acid. Hence, the quantum efficiencies in terms of the single electron transfer steps must be significantly higher than those expressed in term of stearic acid. However, since the degradation of the stearic acid adsorbed on the surface may go via the formation of small and volatile molecules without complete breakdown to CO_2 and H_2O the quantum yield per electron transferred is unlikely

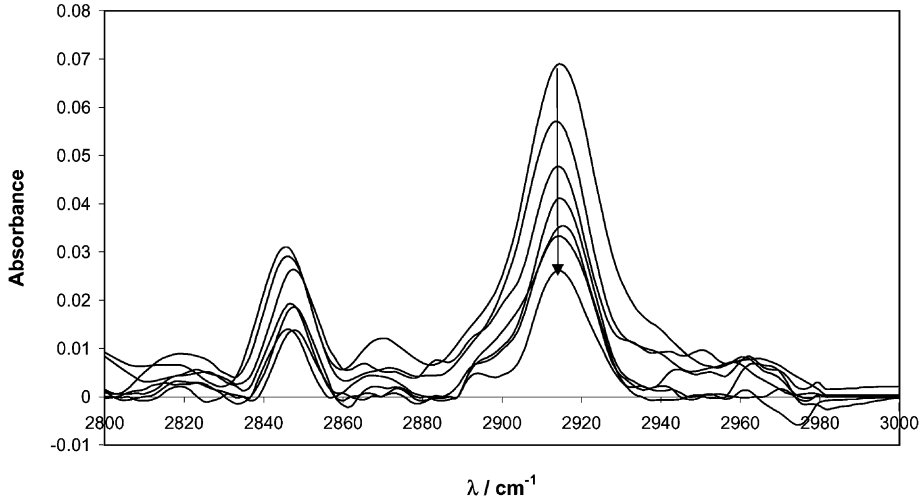

Fig. 12. Loss of absorbance in the C–H stretching region of a stearic acid film on a seven-coat TiO_2 irradiated for 0, 1, 3, 5, 10, 15, and 30 min in direction of arrow.

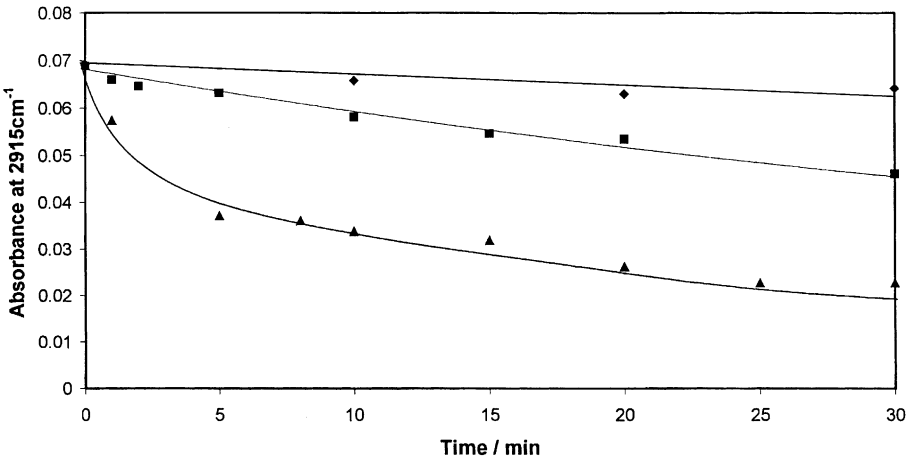

Fig. 13. Degradation profiles for stearic acid on blank (◆), one-coat (■), and seven-coat (▲) spin-coated films.

to be as high as 104 times that calculated on the basis of stearic acid consumption. The initial quantum yields obtained for the one-coat and seven-coat films reported here are significantly higher than those reported earlier.

4. Conclusion

Photochemically active, robust and transparent nanocrystalline thin films of TiO_2 can be made by spin coating onto glass from a sol–gel prepared by hydrolysis of titanium isopropoxide in the presence of ethylene glycols. Characterisation by XRD, SEM and TEM show these films to be smooth deposits of pure anatase crystallites with a particle size of 8–30 nm. Films prepared by dip coating from the sol–gel show similar photochemical activity to those prepared by spin coating. However, dip-coated films are less transparent due to a higher light scattering efficiency and stronger absorption in the visible. In addition dip-coated films have inferior mechanical properties and tend to crack and lift from the glass substrate. Examination by TEM suggests that this is because dip coating results in the retention of a significant amount of the ethylene glycol stabilisers used in the sol–gel preparation.

Quantum yields for the photooxidation of 4-chlorophenol using these spin-coated films are in the range 0.5–1%, and are comparable to those previously reported for similar nanocrystalline films and P25 films [14].

For films of different thicknesses, and therefore different absorption efficiencies, quantum yields for 4-chlorophenol oxidation depend only upon the total number of photons absorbed, i.e. Φ is independent of the absorbed photon flux and charge carrier distribution in the film. By way of contrast, the rate of photoreduction of methylene blue upon these TiO_2 films is independent of film thickness, and quantum yields fall from 1.7 to 0.5% as film thickness (and hence photoabsorption efficiency) is increased, an observation which suggests that this reaction is limited by the surface area of the film.

Since the preparation method used gives pure anatase TiO_2 films, even when soda glass is used as substrate, they show no deleterious sodium ion effect for either 4-chlorophenol oxidation or methylene blue reduction.

These films have a relatively high quantum efficiency for the photooxidation of stearic acid deposited directly onto the film, with $\Phi_{SA} = 1$–3%. This, combined with excellent optical and mechanical properties, suggests that these films may be of particular interest for the development of 'self-cleaning windows'.

Acknowledgements

RF would like to thank EPSRC and Johnson Matthey Technology Centre for financial support via the CASE scheme, and Steve Spratt and Alan Stubbs of Johnson Matthey Technology Centre for XRD, TEM and SEM analyses.

References

[1] A. Mills, S. Le Hunte, J. Photochem. Photobiol. A: Chem. 108 (1997) 1 and references therein.
[2] A. Heller, Acc. Chem. Res. 28 (1995) 503.
[3] Y. Paz, Z. Luo, L. Ragenberg, A. Heller, J. Mater. Res. 10 (1995) 2842.
[4] V. Romeas, P. Pichat, C. Guillard, T. Chopin, C. Lehaut, New J. Chem. 23 (1999) 365.
[5] P. Sawunyama, L. Jiang, A. Fujishima, K. Hashimoto, J. Phys. Chem. B 101 (1997) 11000.
[6] T. Minabe, D. Tryk, P. Sawunyama, Y. Kikuchi, K. Hashimoto, A. Fujishima, J. Photochem. Photobiol. A: Chem. 137 (2000) 53.
[7] A. Heller, S. Sitkiewitz, New J. Chem. 20 (1996) 233.
[8] V. Roméas, P. Pichat, C. Guillard, T. Chopin, C. Lehaut, New J. Chem. 23 (1999) 365.

[9] S. Ushijima, K. Sakamoto, O. Ishitani, J. Adv. Oxidation Technol. 4 (1999) 67.
[10] K. Yoshida, K. Okamura, K. Itoh, M. Murabayashi, Denki Kagaku 66 (1998) 171.
[11] P. Theron, P. Pichat, C. Guillard, C. Petrier, T. Chopin, Phys. Chem. Chem. Phys. 1 (1999) 4663.
[12] M. Bideau, B. Claudel, C. Dubien, L. Faure, H. Kazouan, J. Photochem. Photobiol. A: Chem. 91 (1995) 137.
[13] R.W. Matthews, J. Catal. 111 (1988) 264.
[14] A. Mills, J. Wang, J. Photochem. Photobiol. A: Chem. 108 (1998) 1.
[15] L. Su, Z. Lu, J. Photochem. Photobiol. A: Chem. 107 (1997) 245.
[16] D. Dumitriu, A.R. Bally, C. Ballif, P.E. Schmid, R. Sanjinés, F. Lévy, V.I. Pârvulescu, Appl. Catal. B: Environ. 25 (2000) 83.
[17] H.T. Chang, N.-M. Wu, F. Zhu, Water Res. 34 (2000) 407.
[18] N. Serpone, H. Al-Ekabi, E. Pelizzetti, C. Minero, M.A. Foxe, R.B. Draper, Langmuir 5 (1989) 250.
[19] A.P. Xagas, E. Androulaki, A. Hiskia, P. Falaras, Thin Solid Films 357 (1999) 173.
[20] F. Benoit-Marque, U. Wilkenhoner, V. Simon, A.M. Braun, E. Oliveros, M.-T. Maurette, J. Photochem. Photobiol. A: Chem. 132 (2000) 225.
[21] M. Murabayashi, K. Itoh, K. Togashi, J. Adv. Oxidation Technol. 4 (1999) 71.
[22] O. d'Hennezel, P. Pichat, D.F. Ollis, J. Photochem. Photobiol. A: Chem. 118 (1998) 197.
[23] N. Negishi, T. Iyoda, K. Hashimot, A. Fujishima, Chem. Lett. 9 (1995) 841.
[24] I. Sopyan, M. Watanabe, S. Murasawa, K. Hashimoto, A. Fujishima, J. Photochem. Photobiol. A: Chem. 98 (1996) 79.
[25] J.-S. Kim, K. Itoh, M. Murabayashi, Denki Kagaku 65 (1997) 966.
[26] A. Mills, S. Morris, J. Photochem. Photobiol. A: Chem. 71 (1993) 75.
[27] H. Yoneyama, T. Torimoto, Catal. Today 58 (2000) 133.
[28] A. Mills, S. Morris, R. Davies, J. Photochem. Photobiol. A: Chem. 70 (1993) 183.
[29] A. Mills, R. Davies, D. Worsley, Chem. Soc. Rev. 22 (1993) 417.
[30] A. Mills, R. Davies, J. Photochem. Photobiol. A: Chem. 85 (1995) 173.
[31] R.W. Matthews, J. Phys. Chem. B 91 (1987) 3328.
[32] U. Stafford, K.A. Gray, P.V. Kamat, J. Catal. 167 (1997) 25.
[33] C. Guillard, J. Disdier, J.-M. Herrmann, C. Lehaut, T. Chopin, S. Malato, J. Blanco, Catal. Today 54 (1999) 217.
[34] J. Cunningham, P. Sedlak, J. Photochem. Photobiol. A: Chem. 77 (1994) 255.
[35] A. Mills, J. Wang, J. Photochem. Photobiol. A: Chem. 127 (1999) 123.
[36] S. Naskar, S.A. Pillay, M. Chanda, J. Photochem. Photobiol. A: Chem. 113 (1998) 257.
[37] R.W. Matthews, J. Chem. Soc., Faraday Trans. 1 (85) (1989) 1291.
[38] M. Miyauchi, A. Nakajima, A. Fujishima, K. Hashimoto, T. Watanabe, Chem. Mater. 12 (2000) 3.
[39] M. Grätzel, T. Gerfin, L. Walder, in: G.J. Meyer (Ed.), Progress in Inorganic Chemistry, (1996) Vol. 44.
[40] M. Grätzel, Patent WO 95/29924 Application Example E.
[41] C.G. Hatchard, C.A. Parker, Proc. R. Soc. London, Ser. A 235 (1956) 518–536.
[42] Y. Paz, A. Heller, J. Mater. Res. 12 (1997) 2759.